P2.16

NEAR-SURFACE FLOW REGIMES: RECENT CHANGES AND TOOLS FOR PROGNOSES

S.C. Pryor[1], J.T. Schoof[1] and R.J. Barthelmie[2]

[1] Atmospheric Science Program, Department of Geography, Indiana University, Bloomington, IN 47405
[2] Department of Wind Energy and Atmospheric Physics, Risoe National Laboratory, Roskilde, Denmark

1 Introduction

1.1 Flow regimes in a non-stationary climate

Systematic changes were observed in a range of atmospheric variables over large spatial scales during the twentieth century, but few analyses have focused on quantifying changes in flow regimes despite their importance for climate change impacts on society (Changnon and Changnon 1998; Huang et al. 2001). Analyses of 850 hPa wind speed, as manifest in the NCEP/NCAR Reanalysis fields over the Baltic region, indicated annual mean wind speeds significantly increased (by up to 0.25 m s^{-1}/decade for the annual mean) over the period 1953-1999 (Pryor and Barthelmie 2003). The majority of this increase was associated with increases in the upper quartile of the wind speed distribution and occurred during the winter season. These changes documented by Pryor and Barthelmie 2003) in wind speed are strongly linked to changes in the synoptic scale circulation as manifest in the Grosswetterlagen catalogue and to the recent prevalence of positive phase North Atlantic Oscillation, and hence lead to questions regarding future flow climates.

1.2 Applications and research objectives

Wind farms have typical lifetimes on the order of 30 years, so questions arise regarding the average expected annual energy production (i.e. over the lifetime of the wind farm what is the average expected energy production, or alternatively stated 'what is a normal wind year?'). Recall energy density (E) = $\frac{1}{2}\rho U^3$, where U is wind speed, and that electricity production for most wind turbines only commences as wind speeds exceed approximately 4 m s^{-1}. An additional consideration is the effect of non-stationarities in the global climate system on the evolution of a 'normal wind year' on timescales relevant to wind energy developments.

The research presented herein, is an attempt to address these considerations in the geographic context of the Baltic Sea. Prior to use of GCM simulation output to develop flow and wind energy prognoses over the Baltic it is important to evaluate the performance of the GCMs with respect to the validity of phenomena during the 'present climate'. Hence in this analysis the present climate is represented by the period of overlap between the Reanalysis data sets and the GCM transient simulation (i.e. 1990-2001).

* S.C. Pryor. 812-855-5155. spryor@indiana.edu

The objectives of this research are three-fold:

1. To evaluate if wind speed trends over the Baltic as manifest in the NCEP/NCAR Reanalysis 850 mb flow fields are also evident at other levels and in the ECMWF Reanalysis data.
2. To quantitatively evaluate the ability of a coupled atmosphere-ocean General Circulation Model (HadCM3) to represent the near-surface flow characteristics in the Baltic basin during the first decade of the transient simulation (the 1990's) relative to two Reanalysis data sets.
3. To use the GCM to provide decadal prognoses of flow fields for the twenty-first century for use in a number of environmental applications, but with a specific focus on wind energy resource estimation.

2 Data

The study region is the Baltic basin and, as shown in Figure 1, the study domain extends from approximately 53°N 3.5°E to 65°N 26.5°E. It thus encompasses all areas that are within or adjacent to the Baltic Sea, and is extended to the west to encompass the Norwegian coastline.

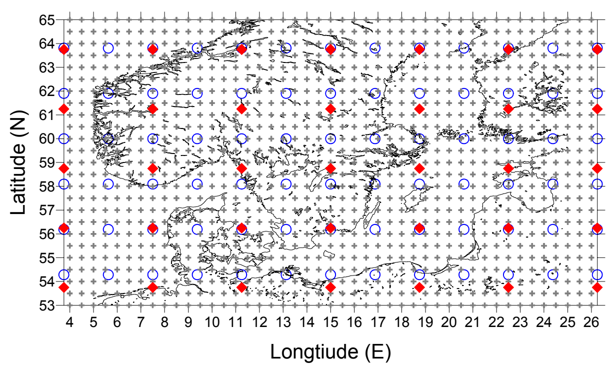

Figure 1. The study domain and grids for the different data sets. + indicate the grid for the ECMWF data. ♦ shows the grid for HadCM3. O indicates the grid for NCEP/NCAR Reanalysis.

2.1 Reanalysis data

Reanalysis projects such as those developed at NCEP/NCAR (Kalnay et al. 1996; Kistler et al. 2001) and the ECMWF (Simmons and Gibson 2000) draw data from a range of sources, which are quality controlled and assimilated with a consistent data simulation system (models). These Reanalysis products thus comprise four-dimensional, homogenized and systematic data sets.

2.1.1 The NCEP/NCAR Reanalysis project

The NCEP/NCAR Reanalysis data are available from 1953 to 2001. Herein we use four-times daily (00, 06, 12, 18 UTC) 10 m wind speeds and direction calculated from the data set wind components (u and v) for each 1.875° x 1.875° grid shown in Figure 1. Figure 2 shows the land-sea mask and land surface type and topography used for the NCEP/NCAR Reanalysis data assimilation model.

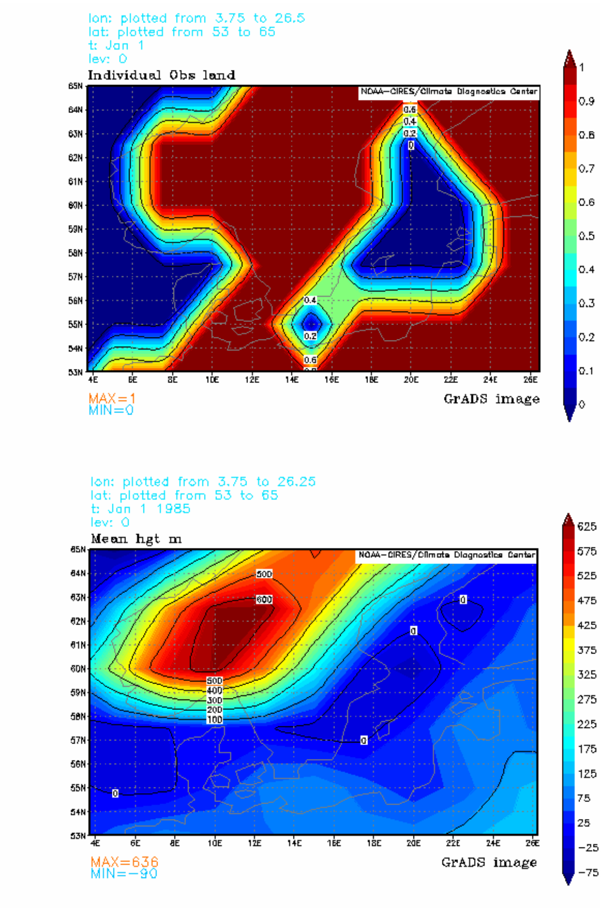

Figure 2. Contoured maps of the NCEP/NCAR Reanalysis grid cell average land fraction (above) and topography (below) from: http://www.cdc.noaa.gov/cdc/data.ncep.reanalysis.html

The atmospheric model used for the NCEP/NCAR Reanalysis project has the following characteristics:

- Horizontal representation is spectral (spherical harmonic basis functions) with transformation to a Gaussian grid for calculation of nonlinear quantities and physics. The horizontal resolution is spectral triangular 254 (T254), and the Gaussian grid is 768 by 384 which is roughly equivalent to a horizontal resolution of 0.5 x 0.5 °. N.B. The data is archived at the coarse resolution described above (of approximately 1.875 x 1.875° for the near-surface flow components).
- The vertical domain is divided into 64 unequally-spaced sigma levels with enhanced resolution near the bottom and the top. For a surface pressure of 1000 hPa, 15 levels are below 800 hPa, and 24 levels are above 100 hPa.

The NCEP/NCAR Reanalysis products are available from: http://www.cdc.noaa.gov/cdc/reanalysis/.

2.1.2 The ECMWF Reanalysis project

The new Reanalysis project at ECMWF ERA-40, covers the period from mid-1957 to 2002, and hence includes the earlier ECMWF Reanalysis ERA-15, 1979-1993. Herein we use four-times daily (00, 06, 12, 18 UTC) 10 m wind speeds and direction calculated from the data set wind components (u and v) for each 0.5° x 0.5° grid shown in Figure 1. The atmospheric model used for ERA-40 has the following characteristics:

- T159 spherical-harmonic representation for basic dynamic fields, with a reduced Gaussian grid of approximately uniform 125 km spacing for surface and other grid-point fields.
- There are 60 levels in the vertical.

The ECMWF Reanalysis data are available from: http://www.ecmwf.int/research/era/.

2.2 General Circulation Model: HadCM3

In this analysis we use daily wind speeds output from the HadCM3 GCM (Johns et al. 1997; Stratton 1999; Pope et al. 2000) transient simulation (1990-2100) for the A2 emission scenario (IPCC 2000). The atmospheric component of HadCM3 has 19 levels with a horizontal resolution of 2.5° of latitude by 3.75° of longitude (Figure 1), which produces a global grid of 96 x 73 grid cells. This is equivalent to a surface resolution of about 417 km x 278 km at the Equator, reducing to 295 km x 278 km at 45° of latitude (comparable to a spectral resolution of T42).

The model output used here was obtained from the Climate Impacts LINK Project (DERFA contract EPG 1/1/124) on behalf of the Hadley Center and U.K. Meteorological Office.

3 Methods

3.1 Comparison of the Reanalysis data sets

Despite the clear utility of the Reanalysis data sets several shortcomings of these data have been documented (Hines et al. 2000; Swail and Cox 2000) and hence there is a recognized need to evaluate the Reanalysis projects relative both to other Reanalysis data sets and to independent data not assimilated within the Reanalysis process (Hastenrath and Polzin 2002; Schoof and Pryor 2003). This is particularly relevant to the current application because near-surface observations of winds over land are not included in the derivation of the NCEP/NCAR Reanalysis data set (Kalnay and Cai 2003), and also in light of analyses (Frank and Mann 2001) which suggest that surface roughness values from Denmark as used in the NCEP/NCAR Reanalysis model (Dorman and Sellers 1989) are biased high leading to underestimation of near-surface wind speeds in the NCEP/NCAR Reanalysis data set relative to in situ measurements.

Near surface flow as manifest in the two Reanalysis data sets was thus compared in terms of:

(a) The mean fields over the period of overlap: January 1958 to December 2001. This analysis is focused on assessment of the degree of correspondence of the mean spatial patterns as manifest in the two data sets.

(b) Trends at grid cells which are coincident or nearly so between the two Reanalysis data sets and HadCM3 (see Table 1) for the period 1958-2001. This analysis is thus focused on assessment of the degree of correspondence of temporal trends as manifest in the two data sets.

Table 1. The location of the co-incident grid cells from the Reanalysis data sets and HadCM3.

Grid #	ECMWF		NCEP		HadCM3	
	Lat (°N)	Long (°E)	Lat (°N)	Long (°E)	Lat (°N)	Long (°E)
A	56	4	56.1893	3.75	56.25	3.75
B	64	4	63.8081	3.75	63.75	3.75
C	56	7.5	56.1893	7.5	56.25	7.5
D	64	7.5	63.8081	7.5	63.75	7.5
E	56	11	56.1893	11.25	56.25	11.25
F	64	11	63.8081	11.25	63.75	11.25
G	56	15	56.1893	15	56.25	15
H	64	15	63.8081	15	63.75	15
I	56	18.5	56.1893	18.75	56.25	18.75
J	64	18.5	63.8081	18.75	63.75	18.75
K	56	22.5	56.1893	22.5	56.25	22.5
L	64	22.5	63.8081	22.5	63.75	22.5
M	56	26	56.1893	26.25	56.25	26.25
N	64	26	63.8081	26.25	63.75	26.25

3.2 Comparison of the Reanalysis data sets and HadCM3 simulations for the 1990's

GCMs exhibit greatest accuracy at large scales and long averaging periods (IPCC 2001). Few studies have evaluated their ability to reproduce near-surface flow which, within the mid-latitudes, is largely determined by pressure gradients, which are in turn a function of the prevailing synoptic scale circulation patterns and interaction with local topographic and land cover conditions. Hence, accurate simulation of near-surface wind speeds requires accurate performance of the GCM across a range of scales and accuracy of boundary conditions.

HadCM3 near surface flow is compared to the two Reanalysis data sets in terms of three characteristics:

(a) Mean wind speed fields derived from daily average data.

(b) Spatial correlations of the flow fields.

(c) Comparisons of wind speed probability distributions for individual grid cells, spatial averages and across the domain.

3.3 Flow prognoses from HadCM3

In this preliminary study, the flow fields from HadCM3 are analyzed with a focus on the upper percentiles of the distribution, since these are intricately linked to the economic feasibility of wind energy. The time series of daily wind speed data from HadCM3 are examined in terms of the temporal trend of the annual 90th percentile wind speed and by decade and grid cell for the period 1990-2040. This time period was selected for analysis because it represents a realistic time horizon for existing and planned wind energy developments. The 90th percentile daily wind speed is calculated for each grid cell and each year 1990-2040 and these data are subject to:

(a) A trend analysis similar to that conducted on the Reanalysis data sets (see section 3.1).

(b) A t-test to compare the mean 90th percentile wind speed from future decades to that of the 1990s. This test provides a first analysis of the degree to which the 1990s are characteristic of the following decades.

4 Results

4.1 Comparison of the Reanalysis data sets

4.1.1 Spatial patterns of mean flow

Mean fields for the 1958-2001 10 m flow fields as manifest in NCEP/NCAR Reanalysis and the ECMWF data set are shown in Figure 3. As shown, the climate of the Baltic is dominated by cyclone passages and hence the study domain constitutes a relatively high wind speed regime. Wind speeds are typically highest in the west of the domain along the coastlines of Norway and Denmark and lowest in the north-east of the domain over Finland and northern Sweden. Wind speeds in the region also show a marked seasonal cycle. They are minimized in summer and maximized in winter.

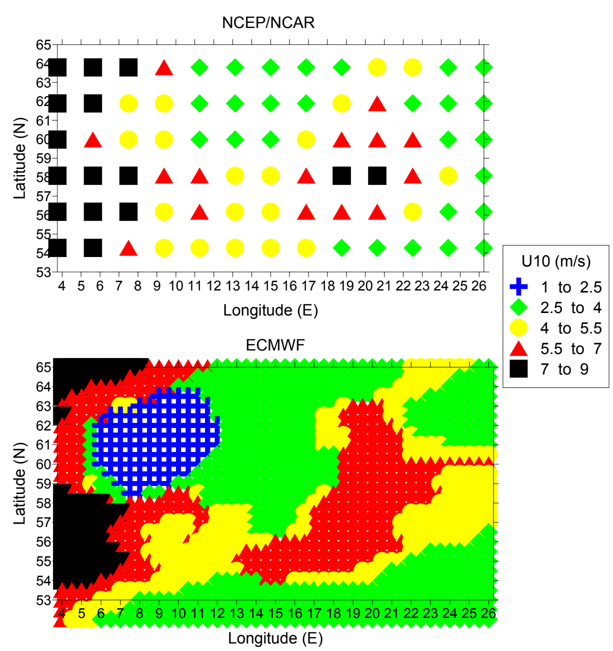

Figure 3. Mean wind speeds 1958-2001 from the NCEP/NCAR and ECMWF Reanalysis data set.

Naturally the ECMWF Reanalysis data set which is the archived at higher spatial resolution exhibits a more complex field than the NCEP/NCAR Reanalysis. The largest discrepancy in terms of the mean wind fields is found in southern Norway where the ECMWF Reanalysis indicates mean wind speeds during 1958-2001 below 2.5 m s^{-1} while the NCEP/NCAR Reanalysis data show values in excess of 2.5 m s^{-1}. This part of the domain is strongly influenced by the Scandic Mountains (see Figure 2) which form the spine of the peninsula on which Sweden and Norway are located and which reach heights of 2,469 m. The differing spatial resolution of the NCEP/NCAR and ECMWF models and data archiving may manifest differing drag and blocking effects caused by this mountain range. The data sets also differ in terms of the wind speeds in the central Baltic Sea (i.e. over water). These portions of the domain exhibit higher wind speeds in the NCEP/NCAR data set than in the ECMWF Reanalysis. Since water has a low and dynamic roughness in the models this would imply higher pressure gradients on average in the NCEP/NCAR Reanalysis data.

4.1.2 Trend analysis

Several geophysical parameters are undergoing changes in the form of the probability distribution as a result of evolution of the climate system due to differential forcing or response of the distribution tails (Robeson 2001; Pryor and Barthelmie 2003) and hence modification in the magnitude or frequency of extreme conditions (Karl and Easterling 1999; Yan et al. 2002). Figure 4 (at the end of this paper) shows the evolution of the annual probability distributions from the NCEP/NCAR and ECMWF data sets for the grid cells shown in Table 1. While there is clear correspondence between the Reanalysis data sets in terms of mutual identification of high wind speed years (e.g. 1982 and 1990), Figure 4 also indicates differences in the probability distributions. For example the six grid cells in the eastern portion of the domain (A-F in Table 1) exhibit higher mean and upper percentiles in the NCEP/NCAR data set. The converse is true for the eastern most grid cells. Two classes of potential causes of this observation can be identified:

1. Differences in the surface parameterizations used in the models. Surface roughness and topography may differ both as a result of differing spatial resolution and data source.
2. Differences in the pressure gradients manifest in the models resulting from, for example, differences in storm tracks.

Differentiating between these two is the subject of ongoing research.

Table 2 shows the results of an analysis of temporal trends in the upper percentile wind speeds. These results are in accord with the findings of earlier work (Pryor and Barthelmie 2003) and emphasize that the latter portion of the C20th was characterized by higher wind speeds in the Baltic region. All grid cells that showed statistically significant wind speed trends showed positive trends in both data sets, although on average the trends were smaller in the ECMWF data. It is worthy of note that the data sets represent grid cell average values, and hence to some degree a trend in the NCEP/NCR data may be more robust since it is representative to a greater area.

Figure 5 shows a 5 year running mean of the annual 10th, 50th and 90th percentile 4 times daily wind speeds for grid cell E (Table 1) over eastern Denmark. This graph illustrates the absence of trends in the lower percentiles and also demonstrates that in both data sets the highest 90th percentile wind seeds occurred in the late 1980s and early 1990s and that the upper percentiles of the wind speed distribution have subsequently declined. This feature is also manifest in observational records from this location (Figure 6), although there is some evidence that the peak in the observational data precedes that in the Reanalysis data, and the absolute values of wind speed differ due to the difference in nominal height in the models and the observational data. As described above this inter-annual and inter-decadal variability of wind speed has particular importance for the wind energy industry.

Table 2. The 'trend' term (m) in regression equations of the annual 90th percentile wind speeds at the grid cells described in Table 1. The regression equations are; y = mx +c, where y is the 90th percentile wind speed in each year, c is the mean 90th percentile wind speed in 1957, m is the trend term (i.e. the increase or decrease in the 90th percentile wind speed in m s^{-1}/yr) and x is the year since 1957. Values are only shown if the 95% confidence intervals on the trend term did not include 0.

Grid #	NCEP	ECMWF
A	0.036	0.026
B	0.029	0.015
C	0.029	0.024
D	0.028	0.017
E	0.018	0.011
F	0.011	0.013
G	0.013	0.014
H	0.009	-
I	0.019	-
J	-	-
K	0.011	-
L	-	-
M	-	-
N	-	-

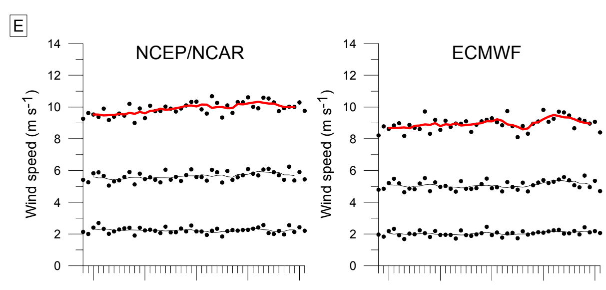

Figure 5. Annual 10th, 50th and 90th percentile wind speeds for grid cell E (over eastern Denmark). Also shown are lines depicting a five year running mean.

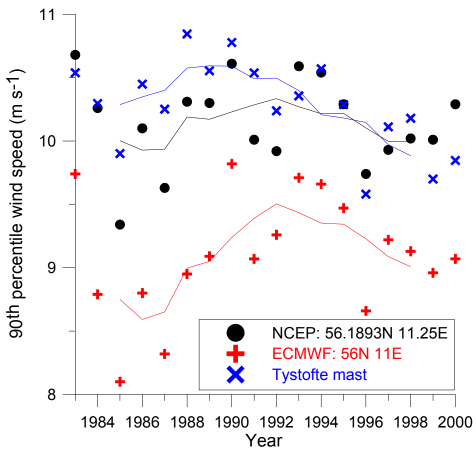

Figure 6. The 90th percentile 4-times daily wind speed from the two Reanalysis data sets for the grid located over eastern Denmark and an observational mast. Note, while the Reanalysis data represent a height of 10 m, the measurement height for the mast is 39.6 m a.g.l. and data are collected as half-hourly average values which have been averaged to generate the four-times daily data used to compute the 90th percentile. The lines indicate a five-year running mean.

4.2 Comparison of HadCM3 and the Reanalysis data sets for 1990-2001

Figure 7 shows the mean daily 10 m wind speed fields from HadCM3 and the Reanalysis data set for 1990-2001. As in Figure 3, the largest discrepancy in terms of the mean wind fields is found in southern Norway where as in the case of the longer data set the ECMWF Reanalysis indicates mean wind speeds during 1990-2001 below 2.5 m s^{-1} while both HadCM3 and the NCEP/NCAR Reanalysis data show values in excess of 2.5 m s^{-1}. As described above this discrepancy may reflect the differing spatial resolution of the models and data archives or it may have a dynamical cause (differences in the tracking or intensity of synoptic scale phenomena in the models).

On average 10 m data from the HadCM3 correctly captures the spatial pattern of mean wind speeds but as shown in Figure 8, the HadCM3 simulated wind speeds are lower in absolute magnitude in the northeast of the domain than those from the two Reanalysis data sets, while the GCM derived wind speeds are slightly higher than those from the Reanalysis data sets over the interior of the Baltic Sea. Further work is required to clarify whether the discrepancies between the HadCM3 and Reanalysis probability distributions of average daily wind speeds are due to spatial filtering as a result of the spatial resolution of the GCM or to dynamical causes. As a first analysis of the importance of the spatial grid resolution, Figure 9 presents the cumulative probability distribution comparisons for an individual grid point, an area average and for the entire grid. The correspondence of wind speeds in grid cell E (over Denmark) between the ECMWF Reanalysis and HadCM3 model is excellent across the entire probability distribution, but over the entire domain HadCM3 overestimates the lower percentile (upto the median) and slightly underestimates the upper percentiles. This bias in the upper percentiles is particularly evident in the winter season when highest wind speeds are typically observed and may imply an underestimation of pressure gradients by HadCM3.

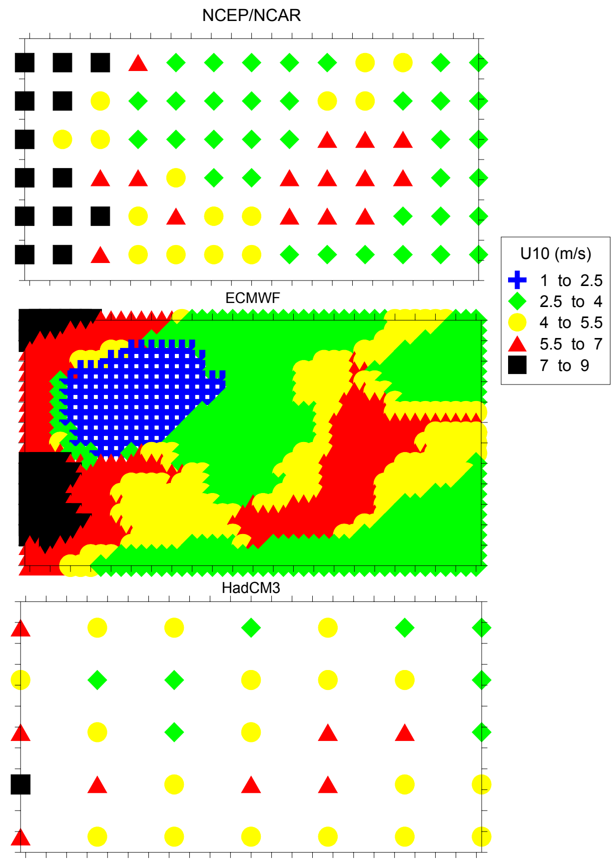

Figure 7. Mean 10 m wind speed from HadCM3 and the two Reanalysis data sets for the period 1990-2001.

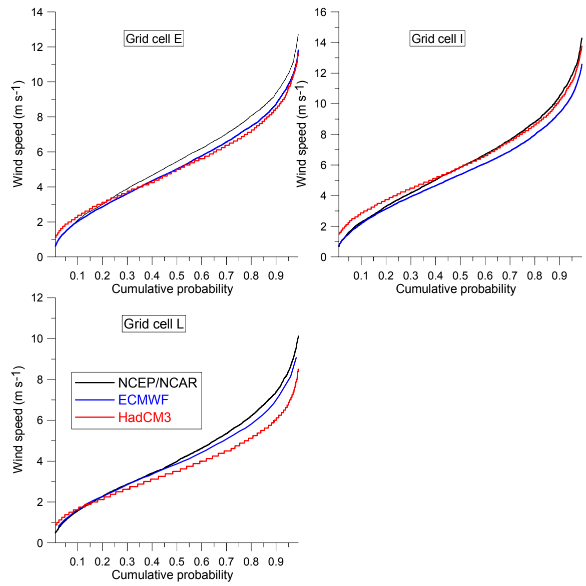

Figure 8. Comparison of the HadCM3 and the NCEP/NCAR and ECMWF Reanalysis 10 m wind speeds for three selected grid cells for the period 1990-2001. Grid cell E is located over eastern Denmark is a region of mixed land-sea surface. Grid cell I is over the interior of the Baltic Sea and hence contains almost exclusive water surfaces in each model. Grid cell L is located in the northeast of the domain over the Finnish coastline.

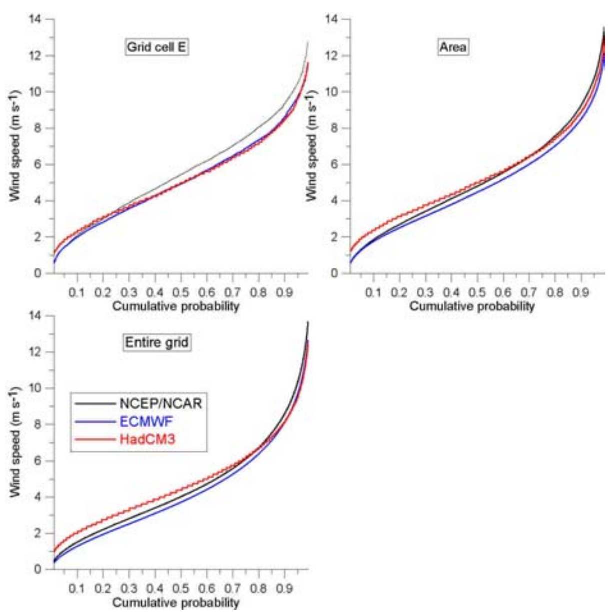

Figure 9. Cumulative probability distributions (1st to 99th percentile) for wind speeds for a range of scales for 1990-2001 from the HadCM3 model and the two Reanalysis data set. Area represents the domain enclosed by: 53-58.4°N, 7.25-13.25°E

4.3 Prognoses of flow from HadCM3

As described above there are some discrepancies between flow regimes as manifest in HadCM3 and those described in the Reanalysis products. Nevertheless assuming that the discrepancies shown above are not also accompanied by biases in the temporal characteristics of HadCM3, we examine HadCM3 in terms of the relative change in flow expected over the forthcoming decades.

The result of the trend analysis over approaching decades is that no grid cell exhibits statistically significant trends in the 90th percentile wind speed over this temporal window. The comparison of the annual 90th percentile wind speed by decade indicated continued decade-to-decade variability with most grid cells exhibiting only statistically insignificant variability. The results for two sample grid cells which encompass Denmark are shown in Table 3. Although a number of decades had a lower mean annual 90th percentile wind speed, the confidence levels associated with the t-statistics are fairly low and do not support assertion of substantial changes in the upper fraction of the wind speed probability distribution over 1990-2040.

Table 3. Results of a t-test conducted to assess the equivalence of means of the 10 90th percentile wind speeds in the specified decades. The word indicates whether the test indicated the later decade had a lower mean than the 1990s (Lower), an equal mean (Equal) or a higher mean (Higher). The number indicates the confidence level associated with each result of the comparison of means test. For each test there are 18 degrees of freedom.

Decade	56.25°N 7.5°E	56.25°N 11.25°E
1990s v 2000s	Lower. 71.3%	Equal. 97.5%
1990s v 2010s	Lower. 91.9%	Lower. 76.8%
1990s v 2020s	Equal. 97.8%	Lower. 81.3%
1990s v 2030s	Lower. 89.2%	Lower. 68.7%

5 Summary

The continued vigor and expansion of wind energy development in the Baltic region is critically dependent on the reliability of the wind resource. Here we provide a first analysis designed to examine the degree to which non-stationarities in the global climate system will or might be manifest as changes in the wind energy resource of the Baltic. This work follows earlier research in which we demonstrated substantial changes in wind speed regimes in this area during the latter portion of the C20th. The ability of GCMs to accurately reproduce near-surface flow has not previously been researched in detail so prior to development of flow prognoses we evaluate Reanalysis data sets and the ability of GCMs to reproduce the flow climate relative to Reanalysis data sets. The results indicate substantial differences both between the Reanalysis products from ECMWF and NCEP/NCAR and between HadCM3 and these products. While differences in spatial resolution may explain some of these discrepancies they are also manifest in fairly homogeneous regions of the domain which may indicate a partly dynamical cause.

6 Acknowledgments

This research was funded in part by a grant from the Nordic Energy Ministry, the STORPARK project funded by the Danish Energy Ministry and a dissertation year fellowship from Indiana University to JTS.

7 References

Changnon, D. and S. A. Changnon (1998): Evaluation of weather catastrophe data for use in climate change investigations. *Climatic Change* **38**: 435-445.

Dorman, J. L. and P. Sellers (1989): A global climatology of albedo, roughness length and stomatal resistance for atmospheric general circulation models as represented by the Simple Biosphere model (SiB). *Journal of Applied Meteorology* **28**: 833-855.

Frank, H. P. and J. Mann (2001): 50 year return wind around Denmark from global reanalysis data. Wind energy for the new millennium. 2001 European wind energy conference and exhibition (EWEC '01), Copenhagen, DK, WIP Renewable Energies, München.

Hastenrath, S. and D. Polzin (2002): Equatorial mid-tropospheric easterly jet over the eastern Pacific: Comparison from the ECMWF and NCEP-NCAR reanalysis. *Journal of Geophysical Research: Atmosphere* **107**: doi: 10/1029/2001JD001394.

Hines, K., D. Bromwich and G. Marshall (2000): Artificial surface pressure trends in the NCEP-NCAR Reanalysis over the Southern Ocean and Antarctica. *Journal of Climate* **13**: 3940-3952.

Huang, Z., D. V. Rosowsky and P. R. Sparks (2001): Hurricane simulation techniques for the evaluation of wind-speeds and expected insurance losses. *Journal of Wind Engineering and Industrial Aerodynamics* **89**: 605-617.

IPCC (2000): Emissions Scenarios. 2000, Cambridge University Press, UK.

IPCC (2001): Climate Change 2001: The scientific basis. Cambridge, U.K., Cambridge University Press.

Johns, T. C., R. E. Carnell, J. F. Crossley, J. M. Gregory, J. F. B. Mitchell, C. a. Senior, S. F. B. Tett and R. A. Wood (1997): The second Hadley Centre coupled ocean-atmosphere GCM: model description, spinup and validation. *Climate Dynamics* **13**: 103-134.

Kalnay, E. and M. Cai (2003): Impact of urbanization and land-use change on climate. *Nature* **423**: 528-531.

Kalnay, E., M. Kanamitsu, R. Kistler, W. Collins, D. Deaven, L. Gandin, M. Iredell, S. Saha, G. White, J. Woollen, et al. (1996): The NCEP/NCAR 40 reanalysis project. *Bulletin of the American Meteorological Society* **77**: 437-471.

Karl, T. R. and D. R. Easterling (1999): Climate extremes: Selected review and future research directions. *Climatic Change* **42**: 309-325.

Kistler, R., E. Kalnay, W. Collins, S. Saha, G. White, J. Woollen, M. Chelliah, W. Ebisuzaki, M. Kanamitsu, V. Kousky, et al. (2001): The NCEP-NCAR 50 year reanalysis: Monthly mean CD-ROM and documentation. *Bulletin of the American Meteorological Society* **82**: 247-267.

Pope, V., M. Gallani, P. Rowntree and R. Stratton (2000): The impact of new physical parameterizations in the Hadley Centre climate model: HadAM3. *Climate Dynamics* **16**: 123-146.

Pryor, S. C. and R. J. Barthelmie (2003): Long term trends in near surface flow over the Baltic. *International Journal of Climatology* **23**: 271-289.

Robeson, S. M. (2001): Increasing growing-season length in Illinois during the 20th century. *Climatic Change* **52**: 219-238.

Schoof, J. T. and S. C. Pryor (2003): Evaluation of the NCEP/NCAR reanalysis in terms of synoptic scale phenomena: A case study from the Midwestern USA. *International Journal of Climatology* **In press**.

Simmons, A. J. and J. K. Gibson (2000). The ERA-40 Project Plan. UK Meteorological Office, UK, available from http://www.ecmwf.int/**:** 63.

Stratton, R. A. (1999): A high resolution AMIP integration using the Hadley Centre model HadAM2b. *Climate Dynamics* **15**: 9-28.

Swail, V. R. and A. T. Cox (2000): On the use of NCEP-NCAR reanalysis surface marine wind fields for a long-term North Atlantic wave hindcast. *Journal of Atmospheric and Oceanic Technology* **17**: 532-545.

Yan, Z., P. D. Jones, T. D. Davies, A. Moberg, H. Berstrom, D. Camuffo, C. Cocho, M. Maugeri, G. R. Demaree, T. Verhoeve, et al. (2002): Trends of extreme temperatures in Europe and China based on daily observations. *Climatic Change* **53**: 355-392.

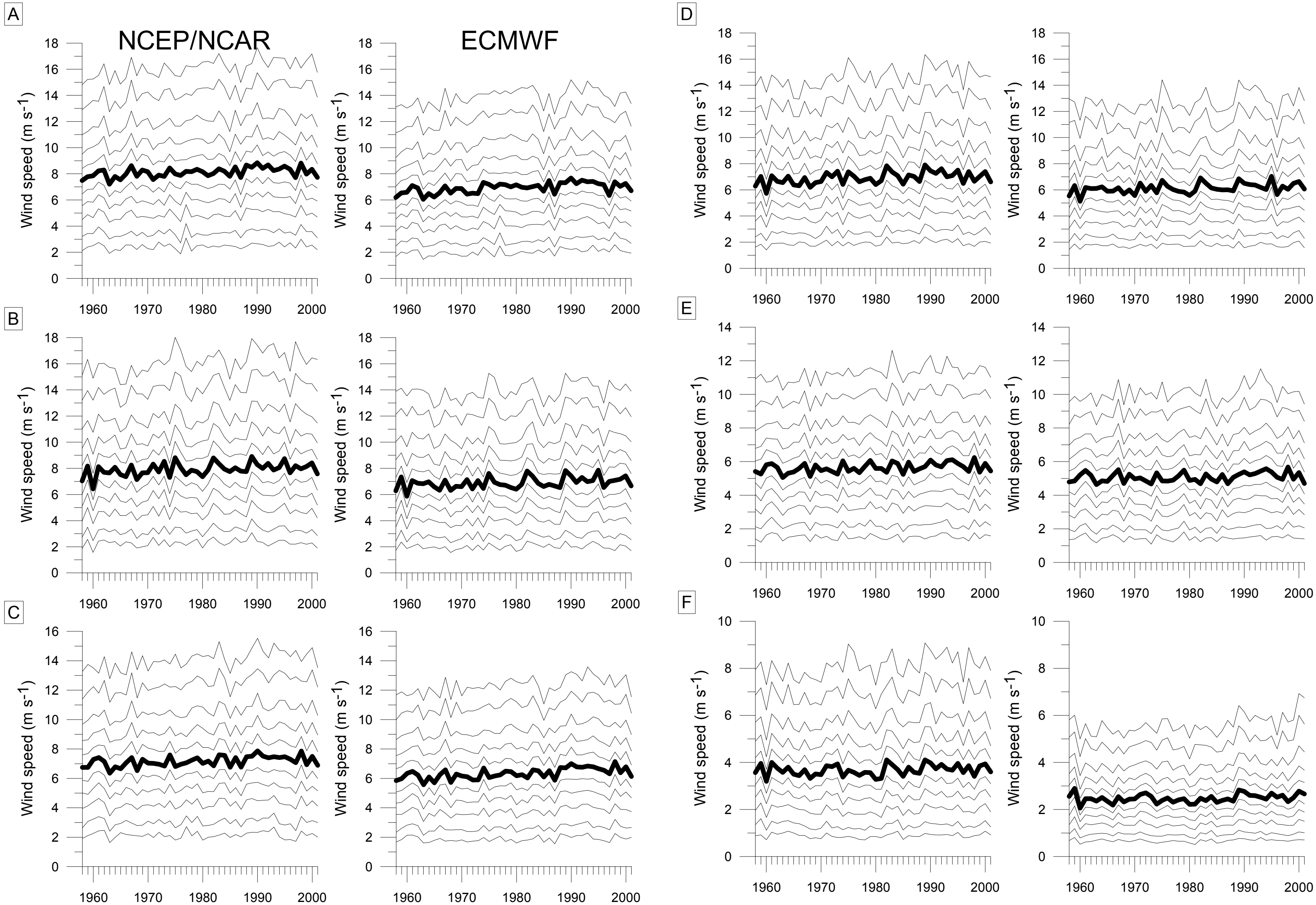
A
NCEP/NCAR
ECMWF
B
C
D
E
F
Wind speed (m s-1)
1960
1970
1980
1990
2000

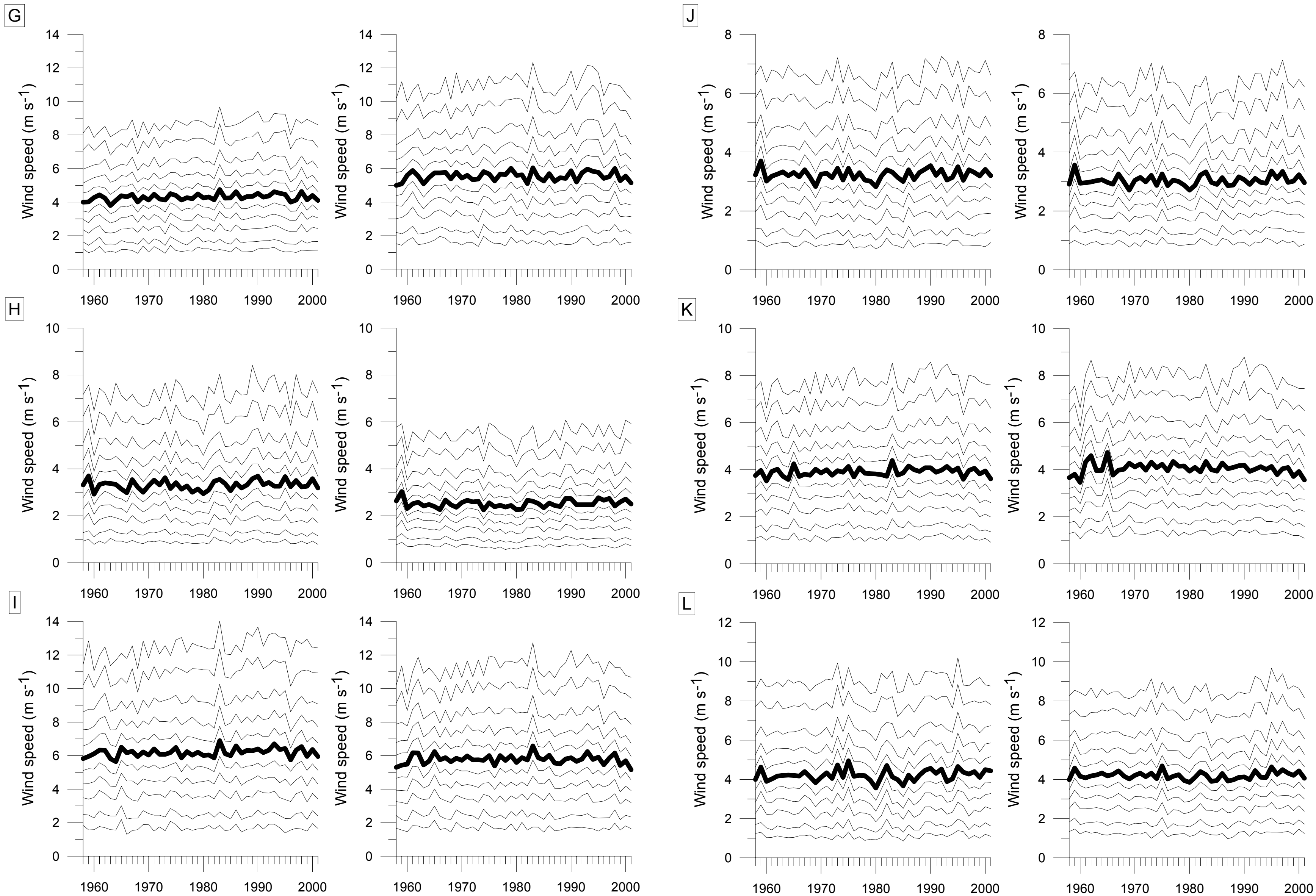

G
H
I
J
K
L
Wind speed (m s-1)
1960
1970
1980
1990
2000

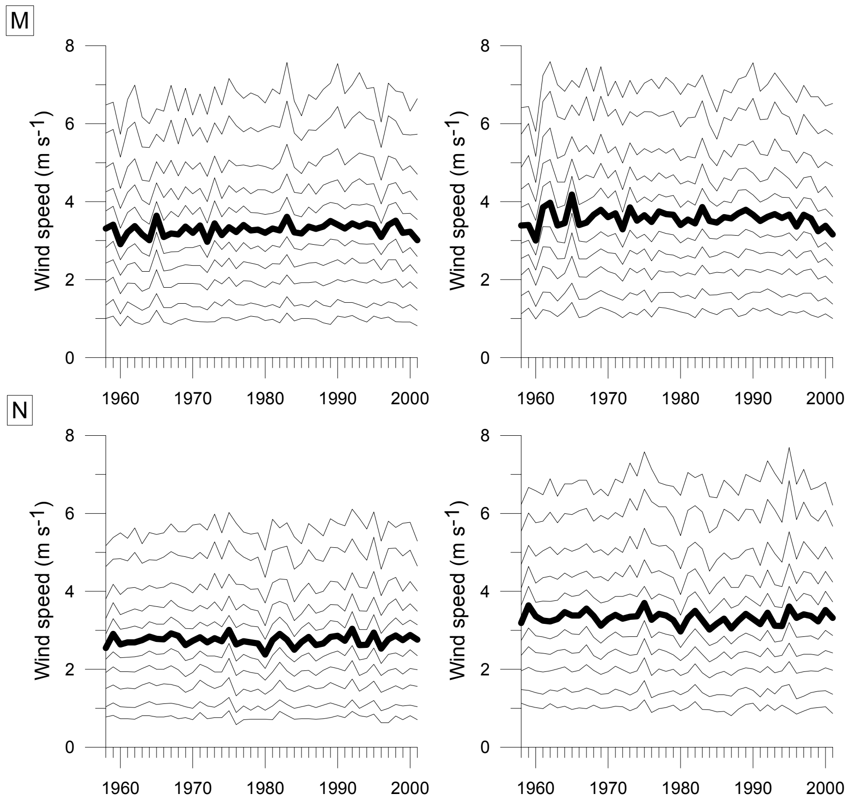

Figure 4. Probability distributions from (left) the NCEP Reanalysis data set and (right) the ECMWF Reanalysis data set, for the proximal grid cells show in Table 1. The lines show the temporal evolution of the 5th, 10th, 20th, 30th, 40th, 50th, 60th, 70th, 80th, 90th and 95th percentiles of the four-times daily 10m wind speed from the annual data sets.